



# FRP fibre-cementitious matrix interfacial bond under time-dependent loading

Mohammed Farooq · Nemkumar Banthia

Received: 20 February 2019 / Accepted: 14 October 2019 / Published online: 17 October 2019  
© RILEM 2019

**Abstract** This paper presents the behavior of the interfacial bond between an innovative FRP fibre and cement mortar under time-dependent loading. Two types of FRP fibres—GFRP and CFRP were investigated. Particularly, the fibre pullout response under quasi-static loading is compared with the response under dynamic loading. To gauge the long term behavior of cracked fibre reinforced composites, fibre relaxation tests were conducted in which initial strain was imparted and sustained, and the relaxation of the composite in terms of drop in load over time period was monitored at room temperature as well as at 50 °C. FRP fibres were found to be to some extent sensitive to loading rate, with an increase in the range of 30–50% in the peak load under dynamic loading. The GFRP fibres itself depicted higher strengths under dynamic loading rate. Under a sustained fibre slip, FRP fibres showed a lower relaxation at both room temperature and at 50 °C compared to commercially available steel and polypropylene fibres. There was also no conclusive change in pullout response in specimen subjected to sustained strains compared to reference.

**Keywords** Fibre reinforced concrete · Fibre reinforced polymers · Dynamic · Relaxation · Impact · Creep

## 1 Introduction and background

A family of innovative FRP fibres with the purpose of use as discrete fibres in concrete were introduced in the previous paper [1]. While several types of FRP fibres were produced and investigated, the best two fibres—unidirectional GFRP and unidirectional CFRP fibres with strength 581 MPa and 953 MPa are discussed in this paper. Vacuum infusion technique was employed to produce FRP laminates of constant thickness and uniformity using unidirectional tapes as reinforcement and epoxy resin. The details of the production methods are explained in the previous paper [1]. These sheets were then cut in direction perpendicular to the direction of reinforcement to 50 mm strips using a bench saw. The FRP strip was further cut in the direction of fibre reinforcement using a guillotine paper cutter as shown in Fig. 1a. Typical CFRP fibers are shown in Fig. 1. A unique surface texture, as shown in Fig. 1c, d was obtained through the vacuum infusion process in which the FRP was cast between two peel plies resulting in the rough texture. The uniformity of the surface texture ( $\sim 280 \mu\text{m}$  peak-to-peak) can be noticed by the measurement from one

---

M. Farooq (✉) · N. Banthia  
Department of Civil Engineering, University of British Columbia, 6250 Applied Science Lane, Vancouver, BC V6T 1Z4, Canada  
e-mail: farooq@alumni.ubc.ca

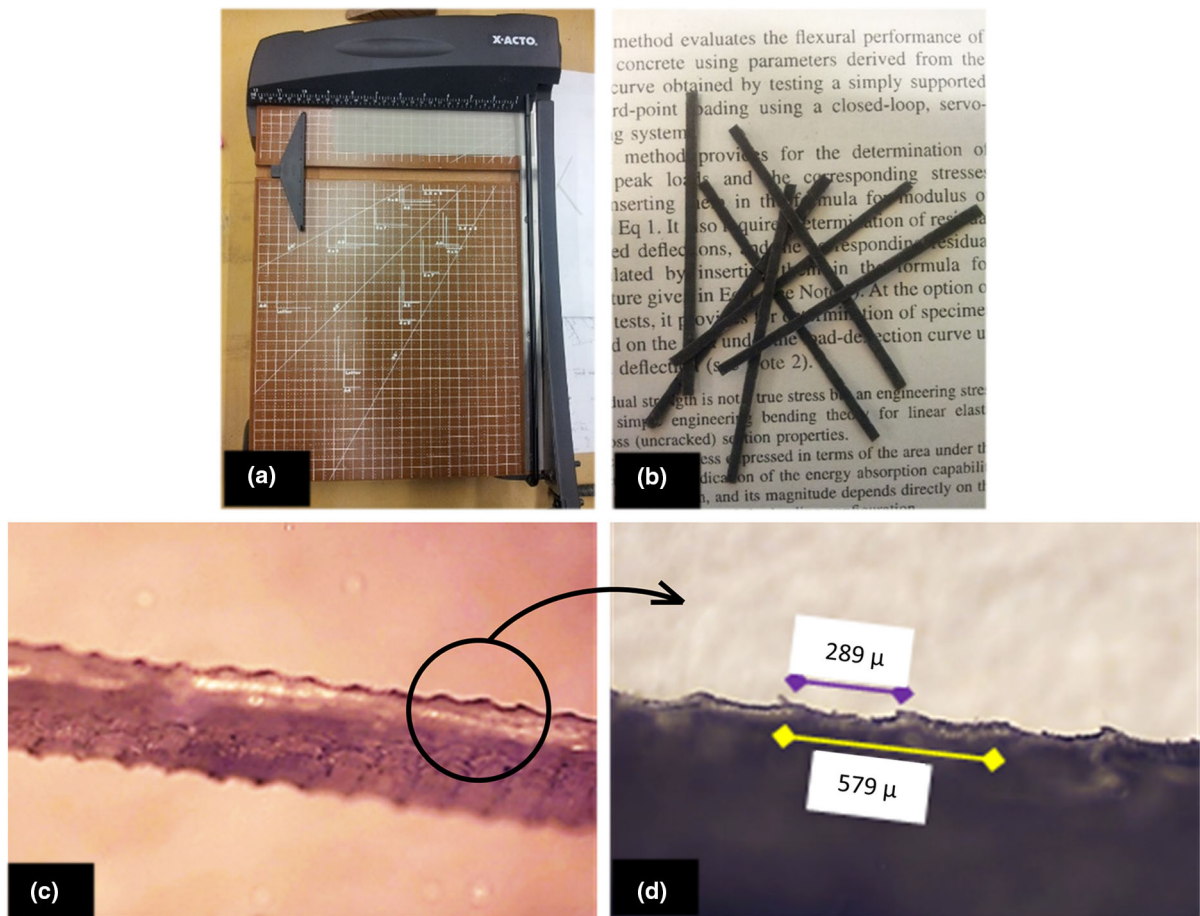


**Fig. 1** Optical microscope images of the profile of a CFRP fibre showing surface deformations

deformation peak to other shown in the figure. Overall it was observed that unidirectional GFRP and CFRP fibres exhibited a superior bond with cementitious matrix in single fibre pullout tests as compared to some of the commercially available steel and polypropylene fibres [1]. Durability tests revealed a drop in tensile strength of GFRP fibres under an accelerated exposure to a high pH environment, but this strength loss was not translated into a reduction in the bond strength with cementitious matrix. CFRP fibres, did not show any noticeable loss of strength or bond under a high pH exposure. The two best performing fibres: uni-directional GFRP fibre and uni-directional CFRP fibre, identified in [1] were chosen for further investigation under time-dependent loading presented in this paper. Henceforth, for ease of reading, these fibres are referred to as GFRP and CFRP fibres respectively.

### 1.1 Rate of loading

Strain rate sensitivities of the fibre-matrix bond-slip behavior are also well researched as obtained by conducting impact tests using a modified Charpy pendulum [2, 3], using drop-weight impact machine [4], using traditional servo-hydraulic systems run at variable rates [5–8] and pneumatic setup [9, 10]. A general increase in the fibre-matrix interfacial bond strength at high rates of loading has been reported. The extent of rate sensitivity as demonstrated by dynamic increase factors (DIF) are however quite scattered [2–5, 7, 11]. Researchers have found fibre-matrix interfacial bond in case of straight smooth fibres to be largely insensitive to the rate of loading [4, 5]. Banthia [5] pointed out the difficulty in conclusively testifying any change in pullout bond strength with small increase in loading rate for smooth straight steel fibres

due the variability, and hypothesized that it is the anchorage mode of load-transfer that could be rate-sensitive. This was confirmed by Xu et al. [8], who reported little change in pullout load for straight steel fibres whereas the fibres with deformation depicted larger pullout resistance for higher rates of loading. Boshoff et al. [12] have on the other hand reported a strong increase in peak pullout resistance with an increase in loading rate for straight PVA micro-fibres (40  $\mu\text{m}$  diameter). Tai et al. [11] also demonstrated rate-sensitivity with increased pullout load and energy for straight steel coated fibres embedded in highly densified ultra-high performance matrix at very high rates of loading, contrary to the initial work for macro steel fibres in regular strength mortar. They attributed this reversal in trend to the highly optimized particle packing in the ultra-high performance matrix. With deformed fibres on the other hand, as much of the load-transfer is through bearing resistance of the deformation (anchorage), a generally higher bond strength under impact loading is reported [2, 13]. Nieuwoudt and Boshoff [13] have also added that this sensitivity to loading rate is due to the deformation in the fibre (hooked end). This increase in pullout load with increased rate of loading has also been proven for polypropylene fibres [14]. For steel fibres, Kim et al. [7] have reported rate-insensitivity for hooked fibres, whereas twisted fibres are reported to show a higher pullout load at a higher loading rate for low, medium and high-strength cement mortar. The rate-sensitivity extends not just to the fibre-matrix interface but FRP fibres itself, which also show sensitivity to different loading rates. In this paper, two dynamic rates of loading and two quasi-static rates of loading were investigated to understand the effect of rate of loading on the FRP fibre-matrix bond.

### 1.2 Long-term reinforcement of cracked section

Under a sustained crack opening, the ability of a fibre to continue to bridge a crack by transfer of load for extended periods of time is critical. Most materials exhibit creep and relaxation i.e. a reduction in stress with time, when the initially deformed strain level is sustained for an extended periods of time. Unfortunately, at the materials level, our current understanding of the individual performances of concrete and fibres does not adequately predict the response of a composite [15, 16]. Recently, the behavior of fibre-

matrix bond under sustained loading has regained some interest [14, 17]. Abrishambaf et al. [18] also showed that for the examined steel fibres with hooked ends, the angle of orientation of the fibre has a major role in the long-term creep of the fibre-matrix interface, with higher angle of orientation depicting a lower creep. This was attributed to the higher pullout resistance due to the friction action. They also reported largely similar pullout behavior obtained from performing pullout tests after long-term creep compared to reference monotonic pullout tests. Nieuwoudt and Boshoff [13] conducted long-term creep tests with the initial load ranging from 30 to 85% of the expected peak load on hooked-end steel fibres. A non-linear increase in amount of creep with initial loading, reason for which was thought to be complex mechanisms involving micro-cracking at large initial load was reported. Here in this paper, short-term single fibre relaxation tests were conducted to understand the response of a fibre while bridging a crack and the crack opening is maintained.

## 2 Experimental programme

The types of FRP fibres: unidirectional GFRP and unidirectional CFRP fibre were investigated in this paper. Their relevant properties are described in Table 1. The FRP fibre-cementitious matrix interfacial bond was assessed by means of single fibre pullout tests performed on dogbone shaped specimen under quasi-static and impact loading. A cement mortar using Type 10 General use cement and sand were used in the ratio 1:1, and a water to cement ratio of 0.35 was employed. Considering the uniform bond model for the sake of simplicity, the interfacial bond stress at a particular crack width opening (say fibre slip 's' during the test) can be obtained by distributing the experimentally obtained load at the fibre slip 'Ps' over the bonded area still embedded in the cementitious matrix. Invariably, the part of the fibre bridging the crack not embedded in the cementitious matrix is subjected to elongation because of the tensile stresses within the fibre. Therefore, the experimentally obtained fibre slip (crack width opening) includes the elongation of the fibre. It is known that the strain of FRP is typically small at 1–2%, and hence this elongation can be neglected compared to the fibre slip.

**Table 1** Properties of unidirectional FRP fibres investigated in the study

	Reinforcing tape	Resin	Length (mm)	Thickness (mm)	Average width (mm)	Volume fraction of fibre in FRP (%)	Average strength (COV)
GFRP fibre	S-2 glass fibre	Epoxy	50	0.4–0.6	1.2	22–30	581 MPa (19%)
CFRP fibre	Carbon fibre	Epoxy	50	0.4–0.8	1.4	32–40	953 MPa (29%)

Thus, using the uniform bond model, the bond stress at any crack opening may be obtained by the Eq. 1.

$$\tau_s = \frac{P_s}{p * (l_f - s)} \quad (1)$$

$P_s$  is the pullout load at slip 's',  $p$  is the perimeter of the fibre,  $l_f$  is the length of the fibre embedded in the matrix at the beginning of the test,  $s$  is the fibre slip (crack opening).

The parameters acquired from the pullout test were: peak interfacial bond strength (Eq. 2), pullout energy (Eq. 3), equivalent bond strength (Eq. 4 [19]), and the mode of failure. The dimensions of each fibre was measured before casting, and bond stress computed based on actual measured dimension.

$$\tau_{\max} = \frac{P_{\max}}{p * l_f} \quad (2)$$

$$E_p = \int_{s=0}^{s_{\max}} P_s \cdot ds \quad (3)$$

$$\tau_{\text{eq}} = \frac{8 * E_p}{p * L_f^2} \quad (4)$$

$\tau_{\max}$  is the maximum bond stress,  $P_{\max}$  is the maximum pullout load,  $s_{\max}$  is the maximum fibre slip (crack opening when pullout load reduces to zero),  $\tau_{\text{eq}}$  is the equivalent bond strength,  $E_p$  is the fibre pullout energy,  $L_f$  is the total length of the fiber, which is twice the embedded length  $l_f$  as dogbone specimen were produced with total length of the fiber equally divided between the two halves of the dogbone.

In all the specimen tested, it was found that in all specimen depicting fibre pullout, the pullout occurred only on one side. It was observed that the maximum fibre slip ( $s$ ) was always less than  $l_f$ , the embedded length under consideration. In other words, the pullout

resistance was reduced to zero before the entire fibre was pulled out of the specimen.

## 2.1 Quasi-static and dynamic loading

Both quasi-static and impact pullout tests were conducted on dogbone specimen at 7 days of curing. Quasi-static tests were conducted on a displacement-controlled screw-driven machine at a loading rate of 0.008 mm/s and 0.08 mm/s rate of loading. Load and displacement were monitored using a load-cell and high-precision LVDT respectively and data acquired at a frequency of 10 Hz. Dynamic fibre pullout tests were performed on similar dogbone shaped fibre pullout specimen on a vertically mounted machine specially fabricated for dynamic pullout tests (Fig. 2) which uses air in a pressurised chamber to generate a uniaxial dynamic load [10]. The machine consisted of a pair of grips for gripping the dogbone shaped fibre pullout specimen as shown in Fig. 3. The top grip was stationary whereas the bottom grip was the bottom grip is pulled down rapidly by an air gun. A dynamic

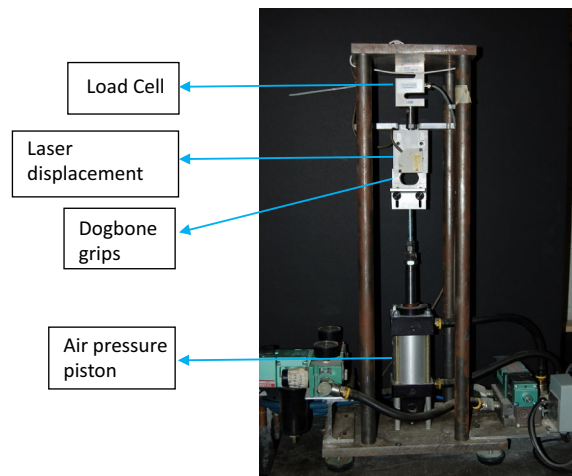


**Fig. 2** Dynamic single fibre pullout setup [10]

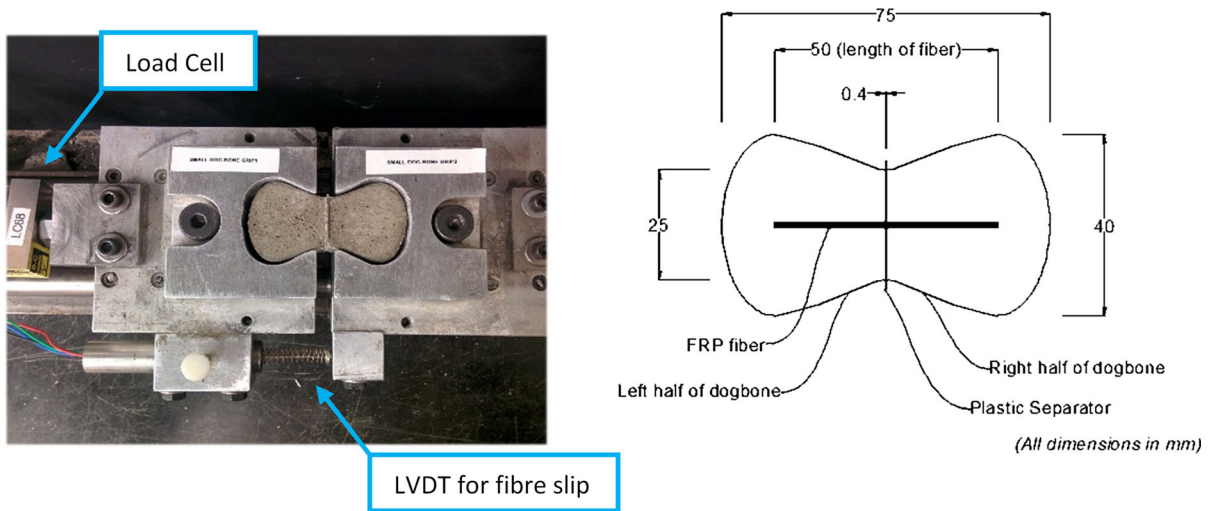


**Fig. 3** Picture of fibre pullout test

load cell with capacity 5 kN was connected to the upper stationary grip to measure the dynamic load. The pressure inside the chamber of the air gun was kept at 2 bar and 20 bar (200 kPa to 2000 kPa), to obtain the two impact loading rates of  $\sim 800$  mm/s and  $\sim 2400$  mm/s respectively. A high precision laser displacement meter was mounted on the grips to record the fibre slip. Both the dynamic load cell and laser displacement meter were interfaced with a high-speed data acquisition system. The dynamic pullout test typically took less than 50 ms and the data was recorded at a sampling rate of 50 kHz. In addition to the pressure inside the air gun, the rate of fibre pullout also depended on the feedback from the specimen resulting in variation of pullout rate. Thus any specimen depicting variation in loading rate in excess of 15% were omitted from the analysis. In both quasi-static and dynamic tests, the recorded load–displacement data was numerically integrated to obtain the area under the curve which is the pullout energy.

For quasi-static tests, at least 10 replicates were tested for each fibre type for a given loading rate. For dynamic tests on the other hand the number of replicates was increased to 25 for each fibre type for each dynamic rate of loading.

## 2.2 Sustained strains and fibre relaxation

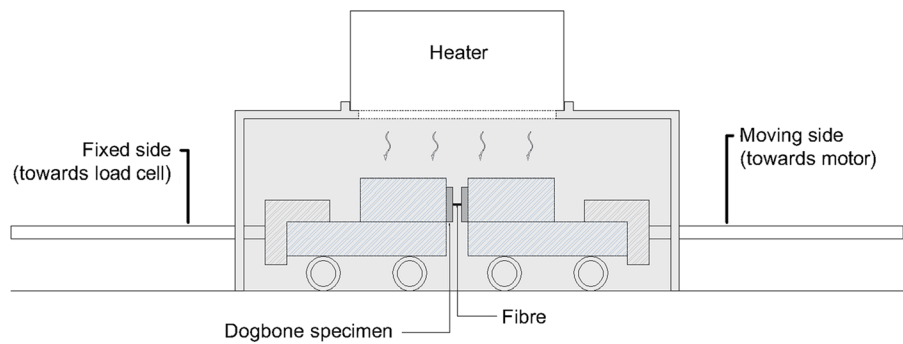
Fibre relaxation tests were performed on the similar dogbone-shaped bonded fibres on the same displacement-controlled fibre pullout setup. Displacement was

imparted until a pullout load about 75% of the expected peak pullout load was achieved, at which time the loading was stopped and the specimen was allowed to relax. Previous studies have shown that a higher initial load results in a higher relaxation of the fibre-matrix interface [16]. Trials were conducted to evaluate relaxation of the FRP fibre-cementitious matrix interface at near-peak load. However, due to the experimental restrictions, a standard pre-load of about 75% of peak load was chosen as the test relaxation load. Relaxation was allowed to occur for 48 h and the drop in load carried by the fibre was monitored. After the relaxation of 48 h, the fibre pullout was resumed to determine the post relaxation performance of the fibre.

In addition to fibre relaxation tests at room temperature, tests were also conducted at an elevated temperature of 50 °C. The setup was modified by adding an external heater that continuously supplied heat and an enclosure to contain the heat within the setup (Fig. 4).

Because the measured relaxation is a combination of the relaxation of fibre-matrix interface and the relaxation of the machine itself, the relaxation of the machine was isolated by conducting a test where the grips were tied to each other and load identical to the ones used for fibre reinforced dogbone specimen was applied. This machine relaxation was experimentally obtained using a solid dogbone specimen, similar to one shown in Fig. 3 but without a fibre or plastic separator. That is, the entire dogbone shaped specimen

**Fig. 4** Schematics of the fibre relaxation setup



was one solid unit. The relaxation test was carried out using this rigid dogbone specimen to obtain the relaxation of the machine and the mortar dogbone specimen. Assuming that the relaxation of machine and FRP fibre-cement matrix interface are independent of each other, the net relaxation of the specimen could be obtained by means of superposition [15, 16]. That is, the net relaxation of the fibre-matrix interface could be obtained by subtracting the experimentally obtained machine relaxation from the experimentally obtained relaxation of the fibre reinforced specimen.

For both—tests at room temperature, and at elevated temperature, four specimen were tested to obtain the average relaxation. In addition to the FRP fibres, hooked-end steel fibres and crimped polypropylene fibres were also tested for comparison.

### 3 Results and discussion

In the single fibre pullout tests, both GFRP- and CFRP fibres depicted a similar load-slip behavior—a linear increase in pullout resistance up to a sharp bend-over point [1]. This bend-over point is believed to be the point of debonding, when the adhesive (chemical) bond between a straight fibre and the matrix is broken [20, 21]. In case of FRP fibres, although they are straight, the uniform surface deformation (roughness) resulting from the manufacturing technique (Fig. 1) provides anchorage at the micro-level. Therefore, the pre-peak ascending portion of the curve represents the pullout resistance due to the combination of the adhesional bond and this mechanical anchorage. The same surface deformations provides an enhanced frictional resistance to pullout once the initial bond is lost.

#### 3.1 Quasi-static and dynamic loading

The load-slip behavior of the GFRP- and CFRP fibre reinforced dogbone specimen are shown in Figs. 5 and 6 respectively, and the bond parameters are summarized in Table 2. Compared to the quasi-static response, at dynamic rates of loading, a small increase of about 31% in case of GFRP fibres, and about 8% in case of CFRP fibres was observed in peak pullout load. While a general increase in peak pullout load is reported by various researchers at dynamic loading rates with polymeric and steel fibres [6, 9], the effect is more pronounced in case of deformed fibres [8]. It is well known that the inability of cracks to coalesce at dynamic loading is the reason for higher failure loads. Xu et al. [8] hypothesized that in the fibre-matrix interface in UHPC, the onset of local micro split-cracking in the matrix in the de-bonded zone—similar to split cracking in pullout of rebar from concrete to be a factor in failure. This is in contrast to the earlier work done by Gokoz and Naaman [4] using smooth fibres in ordinary cement mortar (water to cement ratio = 0.5)

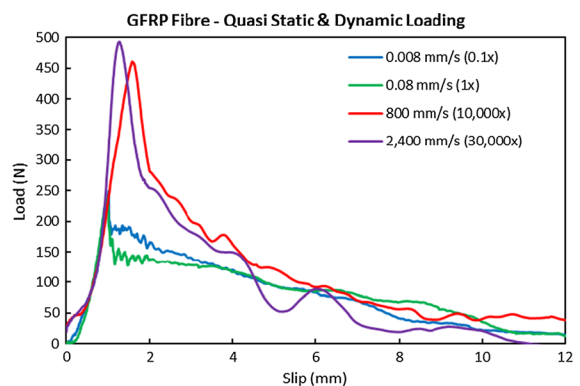


**Fig. 5** Average pullout load-slip graphs of GFRP fibres pullout at different rates of loading

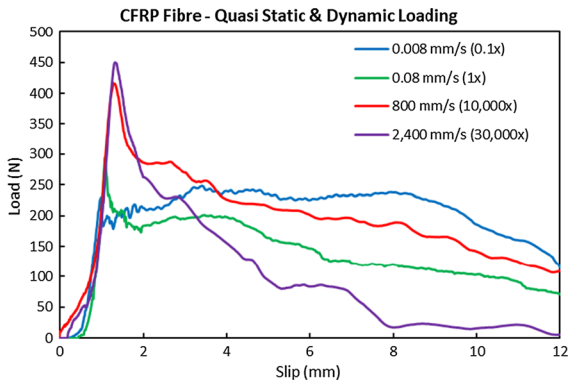


**Fig. 6** Average pullout load-slip graphs of CFRP fibre pullout at different rates of loading

where the fibres could pull out smoothly. Therefore, it seems plausible that whenever the load transferring from the fibre to matrix is considerable enough to cause any cracking in the matrix, rate effects come into play. In the context of deformations on the fibre stressing the matrix around it, FRP fibres present a unique case of surface deformations shown in Fig. 1. This surface deformation results in significant abrasive damage in the tunnel left by the fibre after pullout which is evident from cementitious mortar dust adhering to the fibre after pullout [1]. The rate sensitivity of FRP fibre observed here was considerably smaller compared to the highly deformed steel fibres studied by Banthia and Trottier [2], and highly deformed steel and polymer fibres studied in

Bindiganavile and Banthia [9], and closer to the response of hooked steel fibres observed by Kim et al. [7] and smooth steel fibres observed by Abu-Lebdeh et al. [6], Banthia and Trottier [2] and Xu et al. [8].

Between GFRP and CFRP fibres, GFRP fibres are observed to have a slightly larger sensitivity to the loading rate. Although a marginal increase in peak bond strength at high dynamic loading rate (2400 mm/s) compared to low dynamic loading (800 mm/s) is observed, the two dynamic loading rates demonstrate similar energy absorption at low crack widths. At larger crack widths, a steeper drop in the post-peak pullout load at higher loading-rates led to a lower pullout energy (and equivalent bond strength).

Interestingly, under dynamic rates of loading, none of the GFRP fibre specimen underwent premature fibre rupture, in spite of the fibre stress (~ 700 MPa) exceeding the tensile strength (~ 580 MPa under quasi static conditions). This apparent increase in tensile strength of GFRP fibres is also accompanied by higher tensile strain capacity exceeding the tensile strain capacity at quasi-static conditions as seen from Fig. 5. GFRP itself is known to be strain-rate sensitive, with about 50% increase in tensile strength observed at higher strain-rates by Shokrieh and Omid [22] and 63–89% by Naik et al. [23]. In fact, an increase in their modulus and strain capacity was also reported. An increase in the strength of deformed steel fibres has also been observed in earlier studies on dynamic loading rates by Banthia and Trottier [2] and in

**Table 2** Summary of bond parameters of single FRP fibre pullout at different loading rates

	Loading rate		Peak bond stress <sup>a</sup> (MPa)	Equivalent bond stress (MPa)	Pullout energy (N mm)	Failure mode F: fibre rupture, P: pullout
GFRP fibre	0.008 mm/s	0.1×	2.94 (0.36)	0.91	1026	20% F, 80% P
	0.08 mm/s	1×	3.32 (0.26)	0.94	1054	30% F, 70% P
	800 mm/s	10,000×	4.06 (0.27)	1.02	1080	100% P
	2400 mm/s	30,000×	4.35 (0.25)	0.78	820	100% P
CFRP fibre	0.008 mm/s	0.1×	2.96 (0.27)	2.20	2760	100% P
	0.08 mm/s	1×	3.30 (0.12)	1.72	2109	100% P
	800 mm/s	10,000×	3.3 (0.23)	1.6	2001	100% P
	2400 mm/s	30,000×	3.56 (0.44)	0.75	940	100% P

<sup>a</sup>Standard error in parenthesis



polypropylene fibres by Bindiganavile and Banthia [9]. This increase in tensile strength of GFRP fibres under dynamic loading allowed for fibre pullout in spite of the stronger interfacial bond, averting low-energy brittle fibre rupture. In other words, the rate sensitivity for the FRP fibres was higher than the rate sensitivity of the interfacial bond between FRP fibre and cementitious mortar. This behavior of FRP fibres embedded in cementitious mortars is different from high-strength steel fibres embedded in UHPC mortar investigated by Yoo et al. [24] in which case the rate-sensitivity of steel fibres was lower than that of the interfacial bond, thereby a change in failure pattern from pullout to fibre rupture was noticed. This could be particularly advantageous in composites reinforced with FRP fibres that may be subjected to dynamic or impact loads. Further investigation on flexural and tensile performance of FRP fibre reinforced cementitious composite will have to be carried out to confirm how much improvement will translate from fibre pullout performance to performance of reinforced composite.

### 3.2 Sustained strains and fibre relaxation

The average curves of four specimen of fibre relaxation at room temperature after correction for machine relaxation are shown in Fig. 7. For all fibres, a sudden drop in load transferred by the crack-bridging fibre can be observed immediately at the time loading was stopped. In comparison to the polypropylene fibres, the FRP fibres show by a far lower relaxation under sustained strains. The relaxation of deformed steel fibres in the initial hours was slightly lower than that of

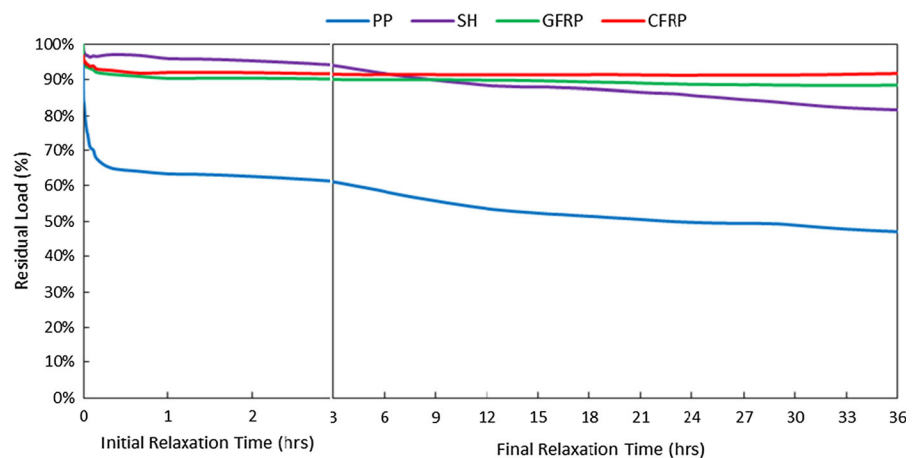
the FRP fibres, but beyond 6 h, the steel fibre continued to relax while the FRP fibre showed little or no further relaxation. Thus indicating that a composite reinforced with FRP fibres could potentially arrest further cracking and prevent collapse of a structural member after a loading event such as seismic or impact over extended periods of time.

It should also be noted that in spite of an up to 30% variation in the peak pullout strength of FRP fibres, the variation in the residual load carrying capacity was within 6% for CFRP fibres and was within 6–7% for GFRP fibres in the initial 20 h, and increased to about 12% at 36 h.

The post-relaxation fibre pullout curves are shown in Fig. 8, and the pullout bond strength and energy absorbed up to 10 mm fibre slip are shown in Table 3. A considerably higher variation in the pullout behaviour was noticeable in the case of the specimen tested after relaxation. A slight improvement in bond strength can be observed for FRP fibres from Fig. 8, however, due to the considerable variability among the four specimens, no definite conclusions can be drawn.

As expected, an overall larger amount of load relaxation for all fibres was observed at 50 °C. At 50 °C, a considerably higher variation in the machine and fibre relaxation curves were observed. While a greater load relaxation was observed for all fibres at higher temperature, steel fibre specimen showed the largest increase in relaxation compared to that at room temperature indicating the influence of elevated temperature (Fig. 9). This is consistent with previous studies have reported large relaxation of steel fibre reinforcing a cracked section [16]. The polypropylene fibres once again exhibited the largest relaxation of all

**Fig. 7** Average load-relaxation curves of polypropylene, steel-hooked, GFRP and CFRP fibres at room temperature





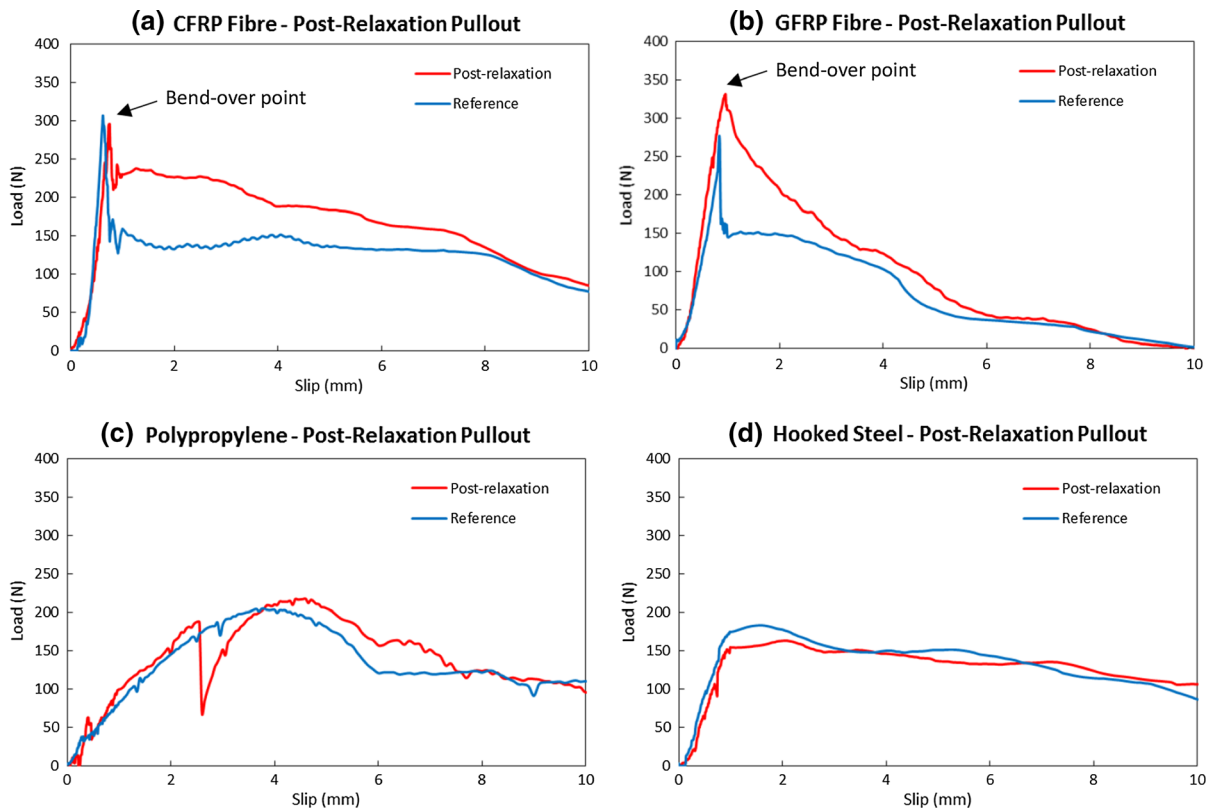


**Fig. 8** Post relaxation pullout curves of different fibres

**Table 3** Pullout behaviour of relaxed specimen

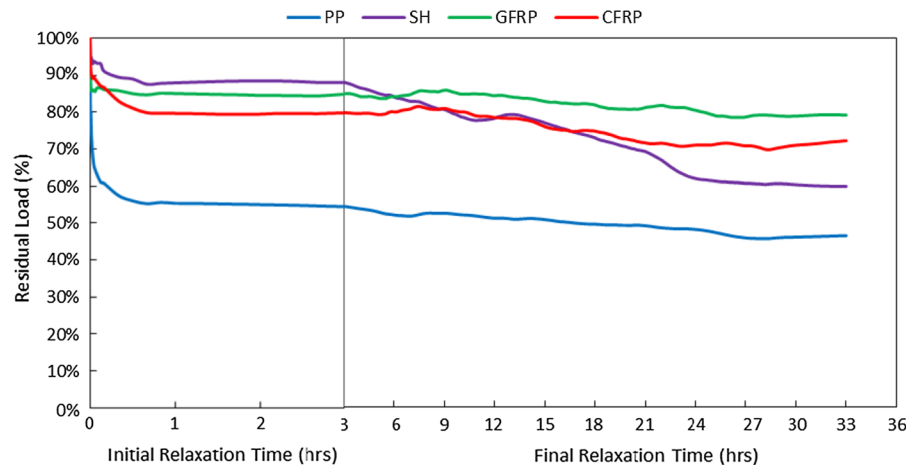
	CFRP		GFRP		SH		PP	
	Post-relax	Ref.	Post-relax	Ref.	Post-relax	Ref.	Post-relax	Ref.
Peak bond stress (MPa)	3.1	3.2	3.9	3.3	3.0	3.4	3.1	2.9
Energy up to 10 mm (N mm)	1817	1397	998	760	1297	1319	1441	1371

fibres, however, the difference between the two temperatures was not as pronounced as the other fibres. The relaxation of the FRP fibres was once again significantly lower than polypropylene fibres and hooked steel fibres. This is likely because of the anchorage between the surface deformations of FRP fibres (Fig. 1) and the cast cement mortar around it. On loading the specimen up to 70% of the peak load, the bend-over point (Fig. 8a, b) in the fibre pullout bond-slip curve marking de-bonding (discussed in detail in earlier paper [1]) is not reached. Therefore, the anchorage because of the surface deformation is still

intact resulting in a recovery of the capacity when the pullout test was resumed after 36 h of relaxation.

The experiments carried out here are only early age trends as from a structure's point of view; and we know that early ages after a major loading event leading to matrix cracking such as earthquakes or impacts are the most critical. Babafemi et al. [17] pointed out that in their long-term creep tests on single fibre pullout (PP fibres), specimen loaded at 50% of their capacity also underwent complete fibre pullout over time. Though from initial studies it appears relatively small relaxation and what looked like 100% recovery was noticed with FRP fibres when the test

**Fig. 9** Average load-relaxation curves of polypropylene, steel-hooked, GFRP and CFRP fibres at elevated temperature



was resumed (Fig. 8), further investigation will have to be done to study the long term effects.

#### 4 Conclusions

A detailed investigation of the interfacial bond between two of newly developed fibres—GFRP- and CFRP fibres and cementitious matrix under different time-dependent loading conditions was carried out in this study. The findings of the study can be concluded as follows:

1. The FRP fibres showed a noticeable strain-sensitivity, with up to 33% increase under dynamic pullout load compared to quasi-static for CFRP fibres. This increase in pullout load in dynamic loading for GFRP fibres was higher, at 48%.
2. Interestingly, no FRP fibres underwent rupture under dynamic conditions, in spite of the stresses in GFRP fibres far exceeded their tensile capacity quasi-static loading, indicating FRP fibres itself are strain-sensitive which worked to our advantage in this study.
3. FRP fibres showed small relaxation under environmental conditions, considerably lower than polypropylene fibres, and slightly better than steel fibres at longer durations.
4. The pullout response of all fibres remained unchanged on application of sustained fibre slip for 48 h.
5. At higher temperature, the relaxation of all fibres increased.

**Acknowledgements** The authors gratefully acknowledge the support received from the Composites Research Network of the Materials Engineering Department at the University of British Columbia. The authors are also grateful for the financial support received from the Tricon Concrete Finishing Company and the Natural Sciences and Engineering Research Council of Canada (NSERC). As well, we wish to show our gratitude for the support given us by the Canada-India Research Centre of Excellence (IC-IMPACTS).

#### Compliance with ethical standards

**Conflict of interest** The authors have no conflict of interest.

#### References

1. Farooq M, Banthia N (2018) An innovative FRP fibre for concrete reinforcement: production of fibre, micromechanics, and durability. *Constr Build Mater* 177C:406–421. <https://doi.org/10.1016/j.conbuildmat.2018.03.198>
2. Banthia N, Trottier JF (1991) Deformed steel fiber-cementitious matrix bond under impact. *Cem Concr Res* 21:158–168. [https://doi.org/10.1016/0008-8846\(91\)90042-G](https://doi.org/10.1016/0008-8846(91)90042-G)
3. Banthia N, Trottier J (1991) Strain rate sensitivity of fibre matrix bond. *Ceram Trans* 16:603–618
4. Gokoz UN, Naaman AE (1981) Effect of strain-rate on the pull-out behaviour of fibres in mortar. *Int J Cem Compos Light Concr* 3:187–202. [https://doi.org/10.1016/0262-5075\(81\)90051-8](https://doi.org/10.1016/0262-5075(81)90051-8)
5. Banthia N (1990) A study of some factors affecting the fiber–matrix bond in steel fiber reinforced concrete. *Can J Civ Eng* 17:610–620. <https://doi.org/10.1139/190-069>
6. Abu-Lebdeh T, Hamoush S, Zornig B (2010) Rate effect on pullout behavior of steel fibers embedded in very-high strength concrete. *Am J Eng Appl Sci* 3:454–463
7. Kim DJ, El-Tawil S, Naaman AE (2008) Loading rate effect on pullout behavior of deformed steel fibers. *ACI Mater J* 105:576–584

8. Xu M, Hallinan B, Wille K (2016) Effect of loading rates on pullout behavior of high strength steel fibers embedded in ultra-high performance concrete. *Cem Concr Compos* 70:98–109. <https://doi.org/10.1016/j.cemconcomp.2016.03.014>
9. Bindiganavile V, Banthia N (2001) Polymer and steel fiber-reinforced cementitious composites under impact loading—part 1: bond-slip response. *ACI Mater J* 98:17–24
10. Bhutta A, Farooq M, Borges PHR, Banthia N (2018) Influence of fiber inclination angle on bond-slip behavior of different alkali-activated composites under dynamic and quasi-static loadings. *Cem Concr Res* 107:236–246. <https://doi.org/10.1016/j.cemconres.2018.02.026>
11. Tai YS, El-Tawil S, Chung TH (2016) Performance of deformed steel fibers embedded in ultra-high performance concrete subjected to various pullout rates. *Cem Concr Res* 89:1–13. <https://doi.org/10.1016/j.cemconres.2016.07.013>
12. Boshoff WP, Mechtcherine V, van Zijl GPAG (2009) Characterising the time-dependant behaviour on the single fibre level of SHCC: part 2: the rate effects on fibre pull-out tests. *Cem Concr Res* 39:787–797. <https://doi.org/10.1016/j.cemconres.2009.06.006>
13. Nieuwoudt PD, Boshoff WP (2017) Time-dependent pull-out behaviour of hooked-end steel fibres in concrete. *Cem Concr Compos* 79:133–147. <https://doi.org/10.1016/j.cemconcomp.2017.02.006>
14. Babafemi AJ, Boshoff WP (2017) Pull-out response of macro synthetic fibre from concrete matrix: effect of loading rate and embedment length. *Constr Build Mater* 135:590–599. <https://doi.org/10.1016/j.conbuildmat.2016.12.160>
15. Banthia N, Krishnadev MR (1990) Steel-fiber cementitious matrix load relaxation studies using a screw-driven testing machine. *Exp Tech* 14:41–43
16. Banthia N, Pigeon M (1989) Load relaxation in steel fibres embedded in cement matrices. *Int J Cem Compos Light Concr* 11:229–234. [https://doi.org/10.1016/0262-5075\(89\)90103-6](https://doi.org/10.1016/0262-5075(89)90103-6)
17. Babafemi AJ, Boshoff WP (2015) Tensile creep of macro-synthetic fibre reinforced concrete (MSFRC) under uniaxial tensile loading. *Cem Concr Compos* 55:62–69. <https://doi.org/10.1016/j.cemconcomp.2014.08.002>
18. Abrishambaf A, Barros JAO, Cunha VMCF, Frazão C (2017) Time dependent behaviour of fibre pull-out in self-compacting concrete. *Cem Concr Compos* 77:14–28. <https://doi.org/10.1016/j.cemconcomp.2016.12.004>
19. Kim DJ, El-Tawil S, Naaman AE (2009) Rate-dependent tensile behavior of high performance fiber reinforced cementitious composites. *Mater Struct* 42:399–414. <https://doi.org/10.1617/s11527-008-9390-x>
20. Kanda T, Li VC (1998) Interface property and apparent strength of high-strength hydrophilic fiber in cement matrix. *J Mater Civ Eng* 10:5–13. [https://doi.org/10.1061/\(ASCE\)0899-1561\(1998\)10:1\(5\)](https://doi.org/10.1061/(ASCE)0899-1561(1998)10:1(5))
21. Naaman AE, Namur G, Najm H, Alwan J (1989) Bond mechanisms in fiber reinforced cement-based composites
22. Shokrieh MM, Omid MJ (2009) Tension behavior of unidirectional glass/epoxy composites under different strain rates. *Compos Struct* 88:595–601. <https://doi.org/10.1016/j.compstruct.2008.06.012>
23. Naik NK, Yernamma P, Thoram NM et al (2010) High strain rate tensile behavior of woven fabric E-glass/epoxy composite. *Polym Test* 29:14–22. <https://doi.org/10.1016/j.polymertesting.2009.08.010>
24. Yoo DY, Kim S (2019) Comparative pullout behavior of half-hooked and commercial steel fibers embedded in UHPC under static and impact loads. *Cem Concr Compos* 97:89–106. <https://doi.org/10.1016/j.cemconcomp.2018.12.023>

**Publisher's Note** Springer Nature remains neutral with regard to jurisdictional claims in published maps and institutional affiliations.

